IEEE Access
Multidisciplinary ⋮ Rapid Review ⋮ Open Access Journal

Received 4 February 2024, accepted 9 March 2024, date of publication 10 April 2024, date of current version 19 April 2024.

Digital Object Identifier 10.1109/ACCESS.2024.3386968

RESEARCH ARTICLE

Hybrid Beamfocusing Architecture and Algorithm for Microwave Wireless Power Transmission Systems

HO YEOL KIM, (Member, IEEE), AND SANGWOOK NAM, (Senior Member, IEEE)
School of Electrical and Computer Engineering, Institute of New Media and Communication, Seoul National University, Seoul 08826, South Korea

Corresponding author: Sangwook Nam (snam@snu.ac.kr)

This work was supported by the Institute of Information & communications Technology Planning & Evaluation (IITP) grant funded by the Korea Government (MSIT) (No.2019-0-00098, Advanced and integrated software development for electromagnetic analysis).

ABSTRACT This study investigates a hybrid beamfocusing method for microwave wireless power transmission (MPT). We propose an optimization algorithm to obtain an optimal coefficient of phase shifters and amplitude controllers with maximum RF power transfer efficiency (RF-PTE) for the hybrid beamfocusing architecture. The optimization algorithm is proposed by iteratively solving the alternative optimization problem. The algorithm is simulated by applying it to an MPT system with a transmitter and receiver composed of patch array antennas operating at 10 GHz. Additionally, we implement a test bed operating at 5.8 GHz. Through the simulations and experiments, the amplitude controllers of partially-connected hybrid beamfocusing architecture can be reduced by half compared with the fully digital beamfocusing to achieve the optimal RF-PTE. Therefore, an economical and less complex MPT system can be implemented by using the hybrid beamfocusing method.

INDEX TERMS Microwave wireless power transmission, optimization algorithm, hybrid beamfocusing, array antenna.

I. INTRODUCTION

Microwave wireless power transmission (MPT) is not limited by the location of the receiver and can charge at a long distance compared with inductive coupling and resonance wireless power transmission. Additionally, it can charge multiple receivers and considers human effects [1], [2]. Therefore, the MPT technology has attracted significant attention for charging many electronic devices and sensors in industries and conferences [3], [4], [5], [6], [7].

In MPT, many studies to maximize power transmission efficiency (PTE) are underway. The overall PTE of an MPT system depends on several efficiencies, such as power source to TX antenna, TX to RX antenna, and RX antenna to received DC power [8], [9]. We investigated the optimization of the PTE of the RF power source to the RX antenna part (RF-PTE). We considered RF signals to maximize the PTE of the MPT system. The methods to determine the optimal signal to transmit maximum power to a receiver include a method using a known channel response and feedback. The optimal amplitude and phase of the transmit signal were obtained using optimization techniques and eigenvalue decomposition in the 5.8 GHz MPT system using known channel response [10], [11]. However, a study that utilizes a feedback algorithm exists. The optimal amplitude and phase of the transmit signal were obtained by transmitting orthogonal matrices with different phases from the transmitter and then feeding back the received power from the receiver to the transmitter. An experiment was conducted by manufacturing an MPT system operating at 10 GHz with a phase array antenna size of a transmitter of 20 × 20 [12]. A beam scanning algorithm that utilizes an iterative method to obtain the optimal phase of the transmit signal was proposed. A 5.8 GHz MPT system that comprises 64 transmit antennas and 16 receive antennas was presented [13]. In these study on MPT, the signal was transmitted by controlling only the phase of the transmit signal or simultaneously controlling the amplitude and phase.

The associate editor coordinating the review of this manuscript and approving it for publication was Tutku Karacolak.

Theoretically, the phase and amplitude of the RF signal applied to each antenna of the transmitter must be controlled to maximize RF-PTE. However, the implementation of the MPT system is limited in terms of cost and complexity when the operating frequency is increased. It can be assumed that a transmit array antenna operating at 24 GHz with a side length of 20 cm (16 wavelengths) and an element spacing of 0.5 wavelengths exists. The number of amplitude controllers and phase shifters that must be connected to each antenna is 1024 same as the number of antennas. Comparing the case of the MPT with the phase-only controlled, an additional 1024 amplitude controllers are needed. The amplitude controllers such as variable gain amplifier (VGA) are expensive at high frequencies because they are active RF components. Therefore, the power consumption and cost of the entire system are significantly increased.

The PTE is not maximum when only the phase of the transmit signal is controlled. However, it is advantageous in terms of cost and system complexity because it does not require components that control amplitude. Additionally, the number of variables is small; thus, less time is required to determine the optimal signal value in practical MPT systems. Consequently, this study aims to determine an algorithm to design an efficient MPT system with low cost, low complexity and high PTE. Therefore, we apply the hybrid beamforming used in communication to the MPT.

In communication, studies on hybrid beamforming, which combines the advantages of analog and digital beamforming, has been researched [14], [15], [16], [17], [18]. Hybrid beamforming is advantageous in terms of cost and system complexity. It can achieve performance close to digital beamforming using fewer RF chains compared with the number of transmit antennas. Generally, the optimal hybrid beamforming architecture is obtained by creating an optimization problem that maximizes spectral efficiency. Hybrid beamforming is divided into two types, partially-connected and fully-connected hybrid beamforming depending on how amplitude and phase are controlled. The spectral efficiency of the latter has the maximum value [19].

This study applies the concept of hybrid beamforming used in communication to MPT. In MPT, the receiver is often located in the radiative near field of the transmitter because transmitter is large to increase power transfer efficiency; therefore, the optimal transmit signal at each antenna has a different phase and amplitude for the power to be focused on the receiver. We define the concept of focusing the power in MPT as beamfocusing.

The category of beamfocusing in MPT is composed of fully-digital beamfocusing, analog beamfocusing and hybrid beamfocusing as shown in Fig. 1. The fully-digital beamfocusing is that control amplitude and phase of transmit signal at each antenna. The optimization algorithm in [10] and [11] is for fully-digital beamfocusing. The analog beamfocusing known as beamforming is that controls only phase of transmit signal. The hybrid beamfocusing is hybrid version of fully-digital and analog beamfocusing. The phase

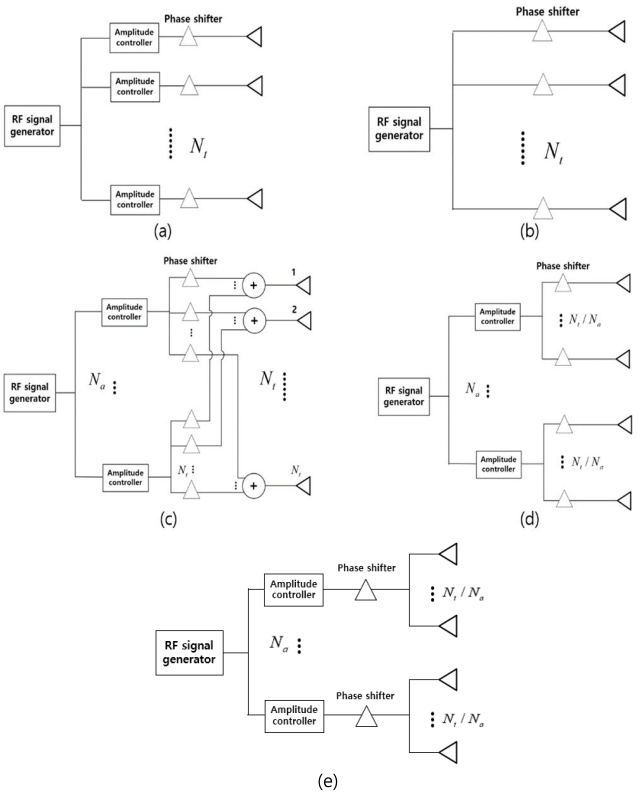

FIGURE 1. Architectures of the MPT system using beamfocusing. (a) Fully digital beamfocusing, (b) Analog beamfocusing (c) Fully-connected beamfocusing (d) Partially-connected beamfocusing (e) Subarray beamfocusing.

of all antennas is controlled and the number of amplitude controllers is smaller than that of antennas. The difference between these architectures is descried in detail in following sections.

We proposed hybrid beamfocusing (HBF) for MPT in this paper and an optimization algorithm to determine the optimal amplitude and phase of the HBF architecture. The optimal RF signal transmitted from each antenna for maximum PTE is obtained using the convex optimization problem [8]. The phase and amplitude of the HBF architecture are obtained by comparing the optimal signal obtained in [8] with the transmit signal in the HBF architecture to minimize the difference. This problem is resolved by dividing the HBF architecture into partially and fully-connected cases. The proposed algorithm was applied to various scenarios of MPT systems operating at 10 GHz and simulated. The performance of HBF was derived. In the given scenarios, the simulation was performed by varying the number of amplitude controllers. Moreover, a partially-connected HBF with fewer amplitude controllers can achieve performance close to the optimal PTE. Further, we propose a subarray beamfocusing architecture to effectively reduce the cost, complexity, and computational load of the system. In addition, we validated the algorithm using an experiment that applies the proposed optimization algorithm to an implemented MPT system operating at 5.8 GHz.

II. OPTIMIZATION PROBLEM FORMULATION

A. FULLY-DIGITAL BEAMFOCUSING ARCHITECTURE

This section provides a brief overview of the fully-digital beamfocusing architecture, which can be used as a comparative reference for HBF. In the case of a fully-digital beamfocusing architecture, each antenna of the transmitter is connected to a phase shifter and amplitude controller, allowing the amplitude and phase of the signal transmitted from all antennas to be adaptively controlled based on the channel, as shown in Fig. 1 (a).

We assumed an MPT scenario using the transmitter and receiver consisting of square planar array antennas. The transmitter and receiver are composed of N_t and N_r antennas, respectively. The received voltage on a receiver at each receiving antenna can be obtained as $V_R(\mathbf{S}) = \mathbf{H}^T\mathbf{S}$ with $\mathbf{H} \in \mathbb{C}^{N_t \times N_r}$ and $\mathbf{S} \in \mathbb{C}^{N_t \times 1}$. The received voltage on multiple receivers, N_m, can be expressed using $\mathbf{H} \in \mathbb{C}^{N_t \times N_r N_m}$. The phase and amplitude of the optimal transmit signal can be obtained using the convex optimization problem proposed in [8].

B. HYBRID BEAMFOCUSING ARCHITECTURE

In a fully connected HBF architecture, each amplitude controller is connected to all antennas; thus, the N_t RF transmitted signals are summed using a power combiner at each antenna, as shown in Fig. 1 (c). In a partially-connect HBF architecture, each N_a amplitude controller is connected to an N_t/N_a number of subarrays, as shown in Fig. 1 (d). The number of amplitude controllers N_a is set to a divisor of N_t such that the ratio N_t/N_a is an integer. The structure of phase shifters in the HBF architecture is known as analog beam-focusers instead of analog beam-formers used in a phased array.

Here, we proposed an optimization problem to obtain the coefficient values of an amplitude controller and a phase shifter that achieve the maximum RF-PTE with the proposed HBF architecture for a given MPT scenario. The RF signal applied by the analog beam-focuser, which is the output signal of the amplitude controller is defined as $\mathbf{x_{RF}} = [x_1, x_2 \cdots x_{Na}]^T$, where $x_n = v_n e^{j\psi_n}$ is the output signal of the *n-th* amplitude controller. v_n and ψ_n are the amplitude and phase of the signal, respectively. The final optimal values of $\mathbf{x_{RF}}$ are real and complex numbers in the case of Fig. 1 (b)-(d) and Fig. 1 (e), respectively. The analog beam-focuser is an $N_t \times N_a$ matrix and is defined differently depending on whether it is partially or fully-connected. In the case of a fully-connected architecture, the values of the matrix elements are complex numbers with a magnitude of 1 with an arbitrary phase. In the case of a partially-connected architecture, the matrix is expressed as follows:

$$\boldsymbol{A} = \begin{bmatrix} \boldsymbol{p}_1 & \mathbf{0} & \cdots & \mathbf{0} \\ \mathbf{0} & \boldsymbol{p}_2 & & \mathbf{0} \\ \vdots & & \ddots & \vdots \\ \mathbf{0} & \mathbf{0} & \cdots & \boldsymbol{p}_{N_a} \end{bmatrix} \tag{1}$$

where $\mathbf{p}_i = \left[\exp\left(j\phi_{(i-1)\frac{N_t}{N_a}+1}\right), \ldots, \exp\left(j\phi_{i\frac{N_t}{N_a}}\right)\right]^T$. The size of $\mathbf{A}$ is $N_t \times N_a$. The transmit signal from the transmit antenna is expressed as $L_{RF}\mathbf{A}\mathbf{x_{RF}}$ by multiplying $\mathbf{x_{RF}}$ by the analog beamfocusing matrix $\mathbf{A}$ and the loss caused by the RF component. L_{RF} is the RF power loss caused in RF components, such as an RF power splitter and combiner. This study defines the phenomenon in which the power of the RF signal is divided into N-ways; thus, the power decreases to one-nth in each RF path as RF loss by the RF power splitter. RF loss by the RF power combiner denotes a decrease in power caused by different phases and amplitudes of RF input signals. L_{RF} is expressed as $\sqrt{N_a/N_t}$ and $1/\sqrt{N_a N_t}$ in the partially and fully-connected cases, respectively. L_{RF} is RF signal loss coefficient regardless of the phase and amplitude of the power combiner input signal and is applied to output signal of amplitude controller. No RF loss was assumed, except for the RF power combiner and splitter. A loss was assumed in the amplitude controller and phase shifter; however, the loss of each product differs and can be compensated for by calibration. The received signal in the receiver is expressed as $L_{RF}\mathbf{H}\mathbf{A}\mathbf{x_{RF}}$ by multiplying a signal transmitted from the transmit antenna by a channel response characteristic. H is the $N_r \times N_t$ channel response. An optimization problem to maximize the receive power and RF-PTE is as follows.

$$\begin{aligned} \max \quad & P_r = |L_{RF}\mathbf{H}\mathbf{A}\mathbf{x_{RF}}|^2, && (2) \\ \text{subject to} \quad & \text{condition of } (\mathbf{A})_{i,j}, \forall i,j && (3) \\ & \mathbf{x_{RF}}^H \mathbf{x_{RF}} \le P_t && (4) \end{aligned}$$

P_r and P_t are received power and transmit power, respectively. Equation (2) is an objective function representing the RF power received from a receiver. Equation (3) is a condition of matrix $\mathbf{A}$ according to the type of HBF architecture, such as partially-connected and fully-connected HBF. Equation (4) is a constraint function to limit the RF transmit power. The aforementioned optimization problem is a multiple variable optimization problem and the element-wise constraints of $\mathbf{A}$; thus, jointly optimizing these two variables is highly complicated. A solution can be obtained with an alternating minimization algorithm that decouples the optimization problem of these two variables [20]. As a principle of alternating minimization, we alternatively solve for $\mathbf{x_{RF}}$ and $\mathbf{A}$ while fixing the others.

Therefore, first, the optimal value $\boldsymbol{y_{opt}}$ to be transmitted from each antenna is obtained using the method proposed in [8]. That is, an optimal transmission signal when the fully-digital beamfocusing is obtained. The optimal value of the HBF can be obtained through a novel optimization problem that minimizes the difference in amplitude between the transmit signal of HBF and $\boldsymbol{y_{opt}}$. Therefore, we propose the objective function of the optimization problem as the square of 2-norm of the difference between the two transmission signals:

$$\min \quad \left|L_{RF}\mathbf{A}\mathbf{x_{RF}} - \boldsymbol{y}_{OPT}\right|_2^2, \tag{5}$$

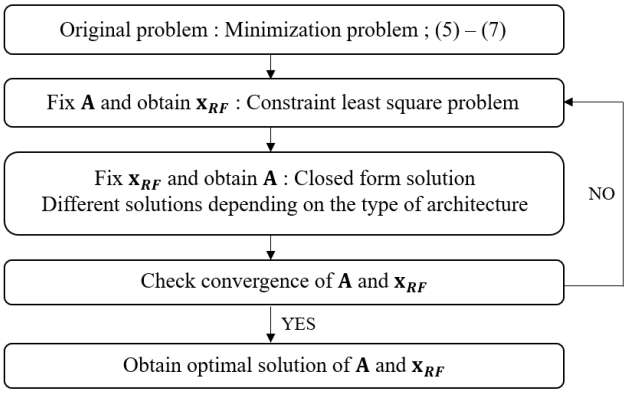

FIGURE 2. Flowchart of the proposed iterative minimization problem.

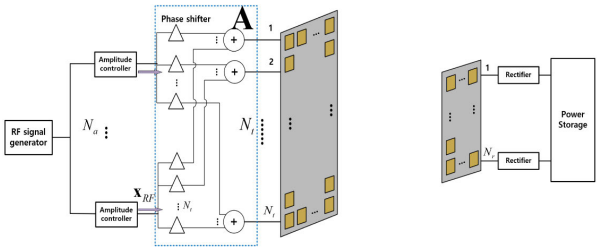

FIGURE 3. MPT system scenario comprising a transmitter and a receiver with an array antenna when the transmitter and the receiver face each other.

$$\text{subject to } (\mathbf{A})_{i,j}, \forall i,j \text{ depending architecture} \tag{6}$$

$$\mathbf{x}_{RF}^{H}\mathbf{x}_{RF} \leq P \tag{7}$$

This optimization problem can be solved using the constraint least square problem if **A** is fixed; $\mathbf{x}_{RF}$ can be obtained. An initial condition of all components of $\mathbf{x}_{RF}$ are set to 1. In case of partially-connected, non-zero components of **A** are set to 1. In case of fully-connected, all components of **A** are set to 1. The constraint least square problem is a convex optimization problem; thus, it is solved using MATLAB and CVX [21]. The **A** structure is defined depending on HBF architectures; **A** of the partially- connected and fully-connected are block diagonal and full matrix, respectively. However, the method for solving problem is the same. Conversely, provided $\mathbf{x}_{RF}$ is fixed, **A** is obtained by a closed form. Therefore, we update **A** and $\mathbf{x}_{RF}$ alternatively until the solution of the optimization problem converges and solve the two problems to obtain the optimal solution. Generally, the solution converges after 3 iterations. **A** is solved differently when $\mathbf{x}_{RF}$ is fixed depending on the **A** structure and the detailed process is as follows.

First, in the fully-connected case, Equation (5) expressed as follows.

$$\min \sum_{i=1}^{N_t} \left| L_{RF} \left(\sum_{j=1}^{N_a} a_{i,j} x_{RF,j} \right) - y_{opt,i} \right|^2 \tag{8}$$

$a_{i,j}$ is the component of matrix **A** with a complex number of magnitude 1. Each term according to i in the first sigma of Equation (8) is independent. Additionally, variables L_{RF}, $x_{RF,j}$, and $y_{opt,i}$ excluding $a_{i,j}$ are fixed values. Therefore, $a_{i,j}$ that minimizes $\left| L_{RF} \left(\sum_{j=1}^{N_a} a_{i,j} x_{RF,j} \right) - y_{opt,i} \right|^2$ can be obtained. $a_{i,j}$ is a complex number with a magnitude of 1, expressed as $e^{j\phi_{i,j}}$. Hence, $x_{RF,j} = \alpha_j e^{j\theta_j}$ and $y_{opt,i} = \beta_i e^{j\psi_i}$ are defined. Substituting the symbols defined in the expression in the first sigma of Equation (8), we obtained:

$$\min \left| L_{RF} \left(\sum_{j=1}^{N_a} \alpha_j e^{j(\phi_{i,j}+\theta_j)} \right) - \beta_i e^{j\psi_i} \right|^2. \tag{9}$$

The methods to minimize this expression are divided into two cases. First, in the case of $L_{RF} \sum_{j=1}^{N_a} \alpha_j < \beta_i$, Equation (9) cannot be equated to zero. Therefore, the phase of the first and second terms should be the same, resulting in a considerably small value. The phase value to satisfy the condition is $\phi_{i,j} = \psi_i - \theta_j$. In the case of $L_{RF} \sum_{j=1}^{N_a} \alpha_j \geq \beta_i$, using the trigonometric formula, Expression (9) can be equated to zero. Consider two complex numbers, $a_i e^{j\Phi_{i,1}}$ and $b_i e^{j\Phi_{i,2}}$, with magnitudes of $a_i = L_{RF}\alpha_1$ and $b_i = L_{RF} \sum_{j=2}^{N_a} \alpha_j$. Suppose $\Phi_{i,1} = \phi_{i,1} + \theta_1$ and $\Phi_{i,2} = \phi_{i,2} + \theta_2 = \ldots = \phi_{i,N_a} + \theta_{N_a}$. In that case, the phases of two complex numbers can be determined for their sum to be $\beta_i e^{j\psi_i}$. Thus, the phase difference between $a_i e^{j\Phi_{i,1}}$ and $b_i e^{j\Phi_{i,2}}$ is determined using the triangular formula as $\omega_i = \cos^{-1}\left[\frac{\beta_i^2 - a_i^2 - b_i^2}{2a_i b_i}\right]$.

Therefore, $a_i e^{j\Phi_{i,1}} + b_i e^{j\Phi_{i,2}}$ can be expressed as $(a_i + b_i e^{j\omega_i})e^{j\tau_i}$. τ_i that satisfies $(a_i + b_i e^{j\omega_i})e^{j\tau_i} = \beta_i e^{j\psi_i}$ is $\psi_i - \gamma_i$, where $\gamma_i = \cos^{-1}\left[\frac{a_i^2 + \beta_i^2 - b_i^2}{2a_i\beta_i}\right]$. Consequently, $\phi_{i,1} = \psi_i - \gamma_i - \theta_1$, $\phi_{i,j} = \omega_i + \psi_i - \gamma_i - \theta_j, j = 2 \ldots N_{RF}$ are obtained.

In the case of a partially-connected architecture, **A** in Equation (1) is substituted into Equation (5) and developed as follows.

$$\min \sum_{i=1}^{N_t} \left| L_{RF} x_{RF,l} e^{j\phi_i} - y_{opt,i} \right|^2 \tag{10}$$

l is defined as the quotient of i/N_a. To minimize the value of (10) when the value of $x_{RF,l}$ is fixed, the value of each term must be minimized because each term in sigma is independent. Thus, the phase of $L_{RF} x_{RF,l} e^{j\phi_i}$ and $y_{opt,i}$ must be equal. Therefore, the optimal phase of partially-connected architecture is obtained as $\phi_i = \psi_i - \theta_l$. The process of solving the proposed optimization problem is shown in Fig. 2. In an analog beamfocusing architecture, an RF signal generator is connected to N_t transmit antennas, as shown in Fig. 1 (b). The solution of analog beamfocusing is obtained when $\mathbf{x}_{RF}$ is 1 in the partially-connected architecture. Finally, **A** which represents the phase of the transmit signal is obtained. In a subarray beamfocusing architecture, the various N_a amplitude controllers and phase shifters are connected to N_t/N_a number of subarrays, as shown in Fig. 1 (e). The solution of subarray beamfocusing is obtained when the components of **A** are given as 1 in the partially-connected architecture. Finally, the vector $\mathbf{x}_{RF}$ composed of complex number is obtained.

III. SIMULATION AND NUMERICAL RESULTS

Here, the RF-PTE according to the number of amplitude controllers was compared. As shown in Fig. 3, it is a scenario in which the transmitter and receiver face each other. The proposed HBF algorithm was applied to the scenario in which the transmitter was 16 × 16 and the receiver was 12 × 12. The transmitter and receiver are faced each other. We compared the fully-digital beamfocusing, analog beamfocusing, partially-connected, fully-connected, and subarray HBF. When the number of amplitude controller is one in partially-connected and fully-connected HBF, RF-PTE of HBF is RF-PTE of analog beamfocusing. The subarray HBF has the same number of phase shifters and amplitude controllers, as shown in Fig. 1 (e). The amplitude and phase of the transmit signal in the common subarray are equal. That is, the number of phase shifters required is the same as the amplitude controller and is reduced compared with that of the partially-connected HBF. For the four scenarios, the number of amplitude controllers is increased by a power of 2, from 1 to 256 and the results of comparing RF-PTE are shown in Figs. 4 and 5. In the first and second scenarios, the receiver is in front of the transmitter and the distance between the two is 0.5 m and 1 m, respectively. In the third scenario, the receiver is located at an angle of 30 ° to the transmitter and the distance between them is 0.5 m; the receiver is facing the center of the transmitter. The last scenario has two receivers, the distance equals 0.5 m at a position of 30 ° twisted in opposite directions.

The maximum RF-PTE of fully-digital beamfocusing was calculated using the algorithm proposed in [8] in MATLAB and CVX. Using the channel estimation method in [8], we can apply estimated channel into the algorithm. Analog beamfocusing is the case in which each antenna signal is the same amplitude and the phase is controlled. The transmitter and receiver are square patch array antennas operating at 10 GHz and the distance between element antennas is 0.6 wavelength. The antenna was designed using CST microwave studio. The active element pattern was obtained using the designed element antenna, the channel between the transmitter and the receiver was obtained, and the RF-PTE was calculated using MATLAB. The rectangular patch antenna is a coaxially fed microstrip patch antenna designed on a Taconic TLY-5 dielectric substrate with a relative dielectric constant of e=2.2, loss tangent of 0.0009, and a dimension of 11.5 mm × 9.59 mm.

The results of simulation are shown in Fig. 4 and 5. In fully-connected HBF, the RF-PTE is constant even when the number of amplitude controllers increases. In a fully-connected structure, the RF power combiner is located in front of each transmit antenna. When RF signals with different amplitudes and phases passing through each phase shifter are combined, RF loss occurs. This results in a smaller RF-PTE. Because RF loss does not occur when signals of the same phase and amplitude are combined in the RF power combiner, the algorithm obtains signals of the same phase and amplitude as the optimal value of fully-connected. That is, the

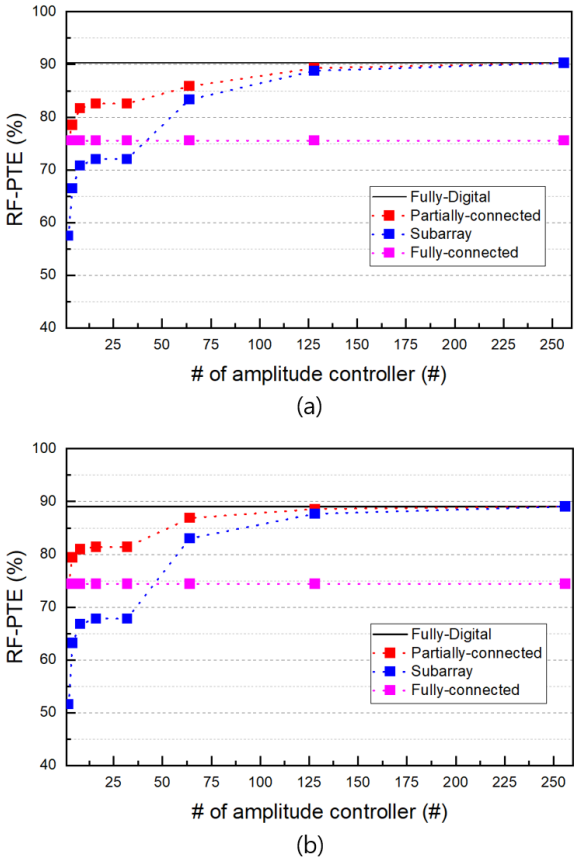

FIGURE 4. Comparison of RF-PTE of hybrid beamfocusing when the number of amplitude controller is increased by power of 2 from 1 to 256. Distance between TX and RX is (a) 0.5m, (b) 1m.

size of each element of $\mathbf{x}_{RF}$ and the phase shifters connected to the amplitude controller are the same regardless of whether the number of amplitude controllers increases. Therefore, the value of the RF-PTE remains unchanged, even if the number of amplitude controllers increases. Conversely, the RF-PTE of partially-connected HBF and subarray HBFs approaches the RF-PTE of the fully digital case as the number of amplitude controllers increases; the value becomes the same when the number of amplitude controllers is 256. Suppose the distance is 1 m. In that case, the RF-PTE values of fully-digital, fully-connected, partially-connected, and subarray with one amplitude controller are 89.0%, 74.4, 74.4%, and 51.6%, respectively. The RF-PTE of analog beamfocusing is 74.4% in this case. In the case of 64 amplitude controllers, the RF-PTEs of partially-connected and subarray are 86.8% and 83%, respectively. Therefore, this result shows that the partially-connected can achieve sub-optimal RF-PTE using amplitude controller as much as 25% of the number of transmitting antennas.

The angle of the receiver of Fig. 5 (a) is tilted by 30 degrees and the efficiencies of Fig. 5 (a) and 4 (a) are almost same. If the receiver is located at a close distance compared to the size of the transmitter, the power transmission efficiency does

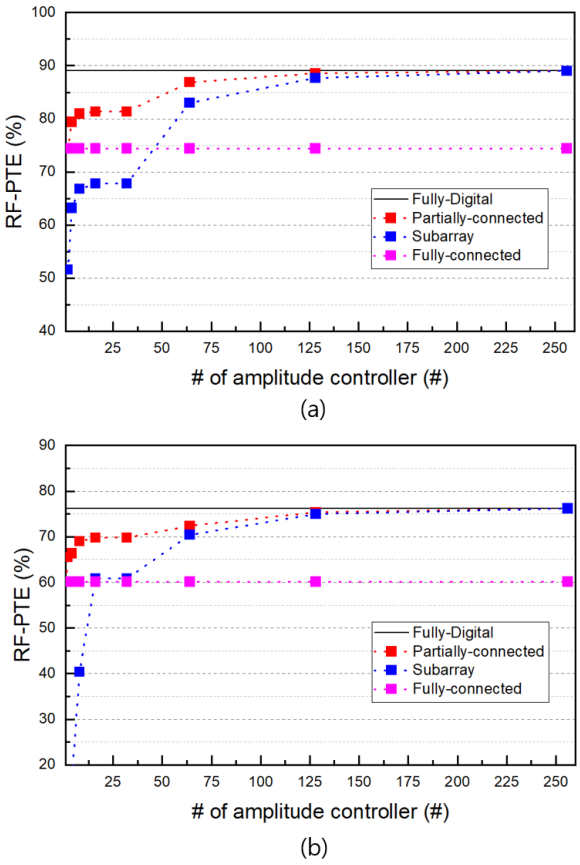

FIGURE 5. Comparison of the RF-PTE of hybrid beamfocusing when the number of amplitude controllers is increased by a power of 2 from 1 to 256. (a) The distance between TX and RX is 0.5 m and the tilted angle is 30 °. (b) Two receivers with a distance of 0.5 m between them, each at a position of 30 ° twisted in opposite directions.

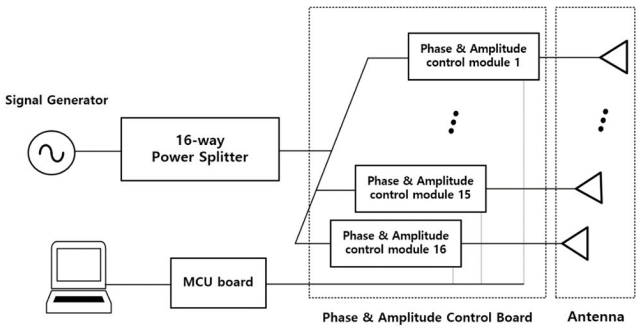

FIGURE 6. Block diagram of the proposed testbed transmit system.

not decrease even if the angle increases. In this case, the size of the transmitter is 28.8cm and the distance is 50 cm. When the distance is close, the tilting angle of the receiver relative to the element antenna does not increase uniformly even if the angle of the receiver is tilted with respect to the center of the transmitter. The tilted angle of element antenna changes differently for each position of the element antenna. Therefore, if the amplitude and phase of each element antenna is optimally controlled by optimization algorithm that we proposed, the power transfer efficiency would be the maximum value.

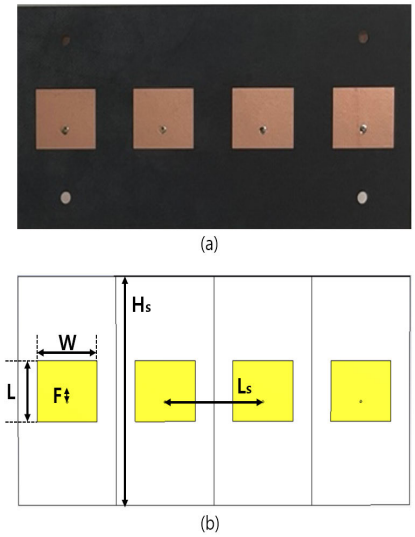

FIGURE 7. (a) Fabricated microstrip patch antenna 4 × 1 (b) Dimension of microstrip patch antenna 4 × 1.

IV. MICROWAVE WIRELESS POWER TRANSMISSION TESTBED DESIGN AND IMPLEMENTATION

This section details the design, structure, and fabrication of all hardware components in the testbed for experimentation. A block diagram of the proposed testbed transmit system is shown in Fig. 6. The implemented MPT system consists of a 16 × 1 patch array antenna transmitter and a 4 × 1 patch array antenna receiver operating at 5.8 GHz. The transmitter includes a signal generator, power splitter, phase/amplitude control board, and patch array antenna, all interconnected via coaxial cables. The power splitter is essential to divide the RF power generated by the signal generator into 16 RF paths. This power splitter comprises two 8-way power splitters and one 2-way power splitter, distributing signals to the 16 RF paths. A phase/amplitude control module is then needed to modify the amplitude and phase of the divided signal. In this study, 16 phase/amplitude control modules were utilized to measure RF-PTE for all cases, ranging from 1 to 16 amplitude controllers of the partially-connected HBF. Each module is designed for digital control and consists of a 7-bit true time delay line and a 5-bit commercial attenuator [21]. The true time delay line provides a 360° coverage of the phase shift value with a resolution of 16° at 5.8 GHz. The attenuator's smallest controllable unit is 0.5 dB, and the largest is 8 dB, capable of attenuating RF power up to 15.5 dB.

Microstrip patch antennas are used for both transmitters and receivers. We conducted an experiment to validate the HBF algorithm proposed in the scenario; thus, the experiment was conducted using an antenna with a basic structure. The layout of the 4 × 1 antenna array with antenna patch dimensions is shown in Fig. 7. The dimensions of the 16 × 1 antenna

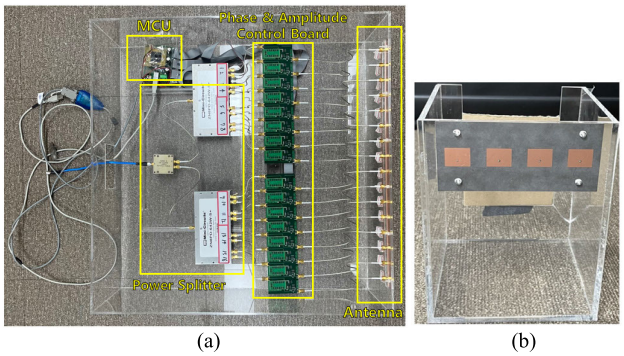

FIGURE 8. (a) Implemented transmit system (b) Implemented receiver.

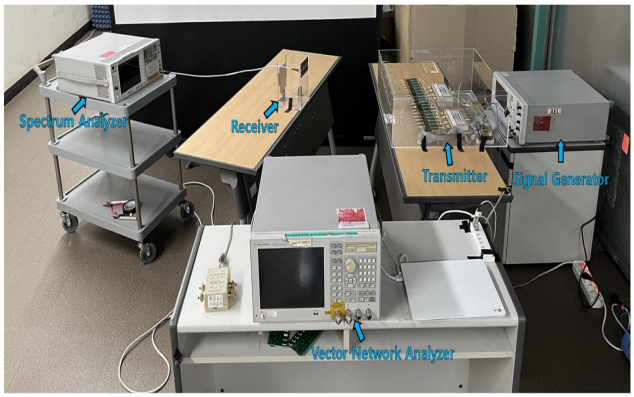

FIGURE 9. Experimental setup of the implemented testbed MPT system.

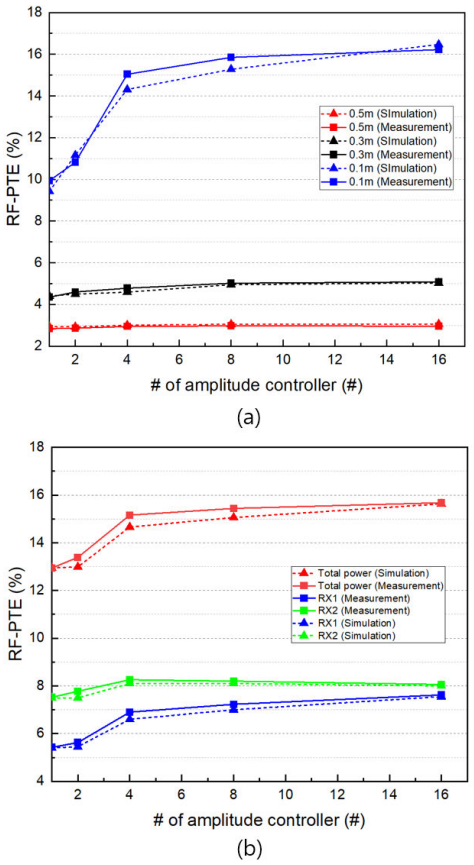

FIGURE 10. Comparison of the RF-PTE in the case of (a) One receiver (b) Two receivers.

array are similar to that of the 4 × 1 antenna arrays. The dimensions of the patch are W = 19 mm and L = 16.5 mm. The spacing between the two patch antenna elements and the vertical length of the substrate are $L_s = 31$ mm and $H_s = 62$ mm, respectively. The distance between the feeding point and the center of the patch antenna is $L_f = 2.9$ mm. The antenna was designed with CST Microwave Studio to operate at 5.8 GHz. Based on the simulation results, the 16 × 1 and 4 × 1 array antennas manufactured on the Duroid 5880 board with a thickness of 30 mil, are shown in Fig. 7. The reflection coefficient of each antenna element was measured using a network analyzer and was lower than -15 dB on all ports. The transmitter system and receiver are implemented as shown in Fig. 8. Each patch antenna was fed to the coaxial feed from the back of the board connected to the transmitter and receiver modules via a coaxial cable.

V. EXPERIMENT RESULT

Here, an experiment was conducted using an MPT testbed manufactured to validate the feasibility of the algorithm, and the resulting experimental data are examined. The experimental setup is shown in Fig. 9. At the transmitter, the signal generator applies the RF signal to the power splitter. Additionally, the micro controller unit (MCU) is connected to the laptop to control the phase and amplitude control board. A vector network analyzer was connected to each receiver antenna to measure a received signal.

First, we measured the S-parameter between the transmitter and the receiver's single antenna using a vector network analyzer to obtain the channel response between them. Next, we utilized the measured channel response in the HBF algorithm, determining the optimal phase and amplitude controller values for each case as the number of amplitude controllers varied from 1 to 16 in powers of 2. Subsequently, we inputted the optimal phase and amplitude values into the phase/amplitude control board of the transmitter through the MCU, enabling the transmission of RF power. The RF power received by the receiver was measured using a spectrum analyzer, and the RF-PTE was calculated based on the measured RF power. The transmit power used in calculating the RF-PTE for the partially-connected HBF in the algorithm is only considered a loss by the power splitter. Therefore, the RF loss of the phase/amplitude control module and cable for each of the 16 paths were measured for calibration. The commercial attenuator introduces a phase difference based on the attenuation state. When calculating the RF-PTE, the amplitude and phase of the RF signal were calibrated, taking into account the RF loss and phase difference between the RF paths.

Experiments were conducted on four scenarios. Three scenarios were when the transmitter and receiver were located in front of each other and the distances between them were 0.1, 0.3, and 0.5 m. The fourth scenario was when the two receivers were located 0.2 m from the transmitter and the angle relative to the transmitter was 30 ° and -30 °, respectively. A graph comparing the RF-PTE of measurement and simulation by varying the number of amplitude controllers from 1 to 16 by powers of 2 for each scenario is shown in Fig. 10.

The simulation and measurement results were in good agreement for all scenarios. Moreover, when the number of amplitude controllers increased, the RF-PTE increased. When the number of amplitude controllers and antennas were the same, the RF-PTEs of full-digital and HBF were equal. The RF-PTE value increased with a decrease in distance. In the case of one amplitude controller and a distance of 0.1 and 0.5 m, the RF-PTEs were 10% and 2.8%, respectively. These results were so because the channel response decreased as the distance increased. With 16 amplitude controllers at a distance of 0.1 m, the RF-PTE increased by 7%. The absolute RF-PTE value would be larger provided the transmitter was larger, indicating that the use of the partially-connected HBF is advantageous in terms of efficiency compared with analog beamfocusing. Additionally, when the number of amplitude controllers was 4, the RF-PTE was 15%, an increase of over 5% compared with the RF-PTE by one amplitude controller. The aforementioned performance was achieved using an amplitude controller of 25% of the total number of antennas, indicating that HBF is highly efficient and can reduce the cost and complexity of the system. As shown in Fig. 10 (b), the total RF-PTE added to the power received from the two receivers and the RF-PTE of each receiver was measured in the case of two receivers. The efficiencies of the two receivers differed in the case of one amplitude controller and became almost the same when the number of amplitude controllers was 16. The magnitude of the efficiency differed because the channels of the two receivers were not symmetrical owing to the asymmetrical nature of the experimental environment, as shown in Fig. 9.

VI. CONCLUSION

This study proposes an optimization algorithm that facilitates efficient MPT by applying the HBF architecture to MPT, determining the optimal values for each phase shifter and amplitude controller. The optimization problem, aimed at achieving maximum RF-PTE in the HBF architecture, involves minimizing the difference between the optimal transmission signal obtained in the fully-digital beamfocusing structure and the transmission signal in the HBF architecture. Additionally, we addressed and resolved the optimization problem for HBF.

We obtained the results by applying the proposed algorithm to various scenarios of an MPT system with an operating frequency of 10 GHz. The transmitter and receiver were equipped with a 16 × 16 and 12 × 12 patch array antenna, respectively. We compared the results of HBF and fully-digital beamfocusing as the number of amplitude controllers increased. The partially-connected RF-PTE validated that an RF-PTE within 4% of the fully digital RF-PTE can be achieved on average using 25% amplitude controllers. Additionally, the subarray architecture demonstrated a high RF-PTE with a relatively small number of amplitude controllers, providing an alternative option for the MPT architecture. When the proposed HBF MPT system was implemented and the optimal signal was obtained with knowledge of the channel, the computational time could be significantly reduced due to the reduced number of variables in use.

The experiment involved designing an MPT testbed system operating at 5.8 GHz to validate the feasibility of the proposed algorithm. A 16 × 1 transmitter patch array antenna and a 4 × 1 receiver patch array antenna were utilized, and the RF-PTE of the partially-connected HBF was measured. This measurement included varying the number of amplitude controllers in various scenarios and comparing the results with simulation results. With an increase in the number of amplitude controllers, RF-PTE exhibited a corresponding increase, achieving values close to those of full-digital beamfocusing with amplitude controllers set at 25–50%. Consequently, the application of partially-connected HBF to MPT demonstrated advantages in terms of cost and complexity. This approach has the potential to establish an MPT system capable of transmitting power with optimal efficiency. Our findings will guide the determination of the structural configuration for future MPT systems during the fabrication process.

REFERENCES

[1] H. Y. Kim and S. Nam, "Optimization of microwave wireless power transmission with specific absorption rate constraint for human safety," *IEEE Trans. Antennas Propag.*, vol. 68, no. 11, pp. 7721–7726, Nov. 2020.
[2] H. Y. Kim and S. Nam, "Efficient microwave wireless power transmission using optimization algorithm," in *Proc. 16th Eur. Conf. Antennas Propag. (EuCAP)*, Mar. 2022, pp. 1–4.
[3] Md. A. Ullah, R. Keshavarz, M. Abolhasan, J. Lipman, K. P. Esselle, and N. Shariati, "A review on antenna technologies for ambient RF energy harvesting and wireless power transfer: Designs, challenges and applications," *IEEE Access*, vol. 10, pp. 17231–17267, 2022.
[4] O. L. A. López, D. Kumar, R. D. Souza, P. Popovski, A. Tölli, and M. Latva-Aho, "Massive MIMO with radio stripes for indoor wireless energy transfer," *IEEE Trans. Wireless Commun.*, vol. 21, no. 9, pp. 7088–7104, Sep. 2022.
[5] O. L. A. López, H. Alves, R. D. Souza, S. Montejo-Sánchez, E. M. G. Fernández, and M. Latva-Aho, "Massive wireless energy transfer: Enabling sustainable IoT toward 6G era," *IEEE Internet Things J.*, vol. 8, no. 11, pp. 8816–8835, Jun. 2021.
[6] M. Tavana, M. Ozger, A. Baltaci, B. Schleicher, D. Schupke, and C. Cavdar, "Wireless power transfer for aircraft IoT applications: System design and measurements," *IEEE Internet Things J.*, vol. 8, no. 15, pp. 11834–11846, Aug. 2021.
[7] S. H. Chae, C. Jeong, and S. H. Lim, "Simultaneous wireless information and power transfer for Internet of Things sensor networks," *IEEE Internet Things J.*, vol. 5, no. 4, pp. 2829–2843, Aug. 2018.
[8] H. Y. Kim, Y. Lee, and S. Nam, "Efficiency bound estimation for a practical microwave and mmWave wireless power transfer system design," *J. Electromagn. Eng. Sci.*, vol. 23, no. 1, pp. 69–74, Jan. 2023.
[9] A. Costanzo and D. Masotti, "Smart solutions in smart spaces: Getting the most from far-field wireless power transfer," *IEEE Microw. Mag.*, vol. 17, no. 5, pp. 30–45, May 2016.

[10] X. Cai, X. Gu, and W. Geyi, "Optimal design of antenna arrays focused on multiple targets," *IEEE Trans. Antennas Propag.*, vol. 68, no. 6, pp. 4593–4603, Jun. 2020.
[11] H. Sun and W. Geyi, "Optimum design of wireless power transmission systems in unknown electromagnetic environments," *IEEE Access*, vol. 5, pp. 20198–20206, 2017.
[12] A. Hajimiri, B. Abiri, F. Bohn, M. Gal-Katziri, and M. H. Manohara, "Dynamic focusing of large arrays for wireless power transfer and beyond," *IEEE J. Solid-State Circuits*, vol. 56, no. 7, pp. 2077–2101, Jul. 2021.
[13] J. H. Park, N. M. Tran, S. I. Hwang, D. I. Kim, and K. W. Choi, "Design and implementation of 5.8 GHz RF wireless power transfer system," *IEEE Access*, vol. 9, pp. 168520–168534, 2021, doi: 10.1109/ACCESS.2021.3138221.
[14] M. Rihan, T. Abed Soliman, C. Xu, L. Huang, and M. I. Dessouky, "Taxonomy and performance evaluation of hybrid beamforming for 5G and beyond systems," *IEEE Access*, vol. 8, pp. 74605–74626, 2020.
[15] S. Payami, M. Khalily, A. Araghi, T. H. Loh, D. Cheadle, K. Nikitopoulos, and R. Tafazolli, "Developing the first mmWave fully-connected hybrid beamformer with a large antenna array," *IEEE Access*, vol. 8, pp. 141282–141291, 2020.
[16] I. Ahmed, H. Khammari, A. Shahid, A. Musa, K. S. Kim, E. De Poorter, and I. Moerman, "A survey on hybrid beamforming techniques in 5G: Architecture and system model perspectives," *IEEE Commun. Surveys Tuts.*, vol. 20, no. 4, pp. 3060–3097, 4th Quart., 2018.
[17] A. F. Molisch, V. V. Ratnam, S. Han, Z. Li, S. L. H. Nguyen, L. Li, and K. Haneda, "Hybrid beamforming for massive MIMO: A survey," *IEEE Commun. Mag.*, vol. 55, no. 9, pp. 134–141, Sep. 2017.
[18] Y. Hu, J. Zhan, Z. H. Jiang, C. Yu, and W. Hong, "An orthogonal hybrid analog–digital multibeam antenna array for millimeter-wave massive MIMO systems," *IEEE Trans. Antennas Propag.*, vol. 69, no. 3, pp. 1393–1403, Mar. 2021.
[19] X. Yu, J.-C. Shen, J. Zhang, and K. B. Letaief, "Alternating minimization algorithms for hybrid precoding in millimeter wave MIMO systems," *IEEE J. Sel. Topics Signal Process.*, vol. 10, no. 3, pp. 485–500, Apr. 2016.
[20] O. E. Ayach, S. Rajagopal, S. Abu-Surra, Z. Pi, and R. W. Heath, "Spatially sparse precoding in millimeter wave MIMO systems," *IEEE Trans. Wireless Commun.*, vol. 13, no. 3, pp. 1499–1513, Mar. 2014.
[21] M. Grant, S. Boyd, and Y. Ye. (2015). *CVX: MATLAB Software for Disciplined Convex Programming*. [Online]. Available: http://cvxr.com/cvx/
[22] M. Yoon and S. Nam, "7-bit multilayer true-time delay up to 1016ps for wideband phased array antenna," *IEICE Trans. Electron.*, vol. 102, no. 8, pp. 622–626, Aug. 2019.

HO YEOL KIM (Member, IEEE) received the B.S. degree in semiconductor system engineering from the University of Sungkyunkwan, Suwon, in 2016, and the Ph.D. degree from the Department of Electrical Engineering and Computer Science, Seoul National University, Seoul, in 2023.

Since 2023, he has been a Staff Engineer with S.LSI, Samsung Electronics. His research interests include microwave wireless power transmission, optimization algorithm, and radar systems.

SANGWOOK NAM (Senior Member, IEEE) received the B.S. degree in electrical engineering from Seoul National University, Seoul, South Korea, in 1981, the M.S. degree in electrical engineering from Korea Advanced Institute of Science and Technology (KAIST), Seoul, in 1983, and the Ph.D. degree in electrical engineering from The University of Texas at Austin, Austin, TX, USA, in 1989. From 1983 to 1986, he was a Researcher with the Gold Star Central Research Laboratory, Seoul. Since 1990, he has been a Professor with the School of Electrical Engineering and Computer Science, Seoul National University. His research interests include analysis/design of electromagnetic (EM) structures, antennas, and microwave active/passive circuits.